IUST
Iran University of Science and Technology

Iranian Journal of Electrical and Electronic Engineering

Journal Homepage: ijeee.iust.ac.ir

Deep Learning for Identification Malaria Diseases from Microscopic Image

Edy Victor Haryanto S*(C.A.), Aimi Salihah Abdul Nasir**, Mohd Yusoff Mashor**, Bob Subhan Riza*, Zeehaida Mohamed***

Abstract: Malaria is a parasitic disease that causes significant morbidity and mortality worldwide. Early diagnosis and treatment are crucial for preventing complications and improving patient outcomes. Microscopic examination of blood smears remains the gold standard for malaria diagnosis, but it is time-consuming and requires skilled technicians. Deep learning has emerged as a promising tool for automated image analysis, including malaria diagnosis. In this study, we propose a novel approach for identifying malaria parasites in microscopic images using the GoogLeNet. Our method includes enhancement with the AGCS method, color transformation with grayscale, adaptive thresholding for segmentation, extraction, and GoogLeNet-based classification. We evaluated our method on a dataset of malaria blood smear images and achieved an accuracy of 95%, demonstrating the potential of GoogLeNet for automated malaria diagnosis.

Keywords: Malaria diseases, deep learning, microscopic image, identification

1 Introduction

MALARIA is a significant health issue in developing nations [1]. Malaria is a parasitic disease endemic in tropical and subtropical regions, with an estimated 247 million clinical cases and 619,000 deaths worldwide in 2021 [2]. The bite of an infected mosquito may transmit Plasmodium parasites into the human body, resulting in the potentially fatal infectious disease known as malaria [3]. Compared to non-pregnant women, pregnant women, fetuses, and newborns are especially susceptible to malaria complications and mortality. An infection with malaria during pregnancy might have detrimental effects on both mother and child [4]. With the assistance of medical professionals, the current method of controlling malaria requires smear microscopy, rapid diagnostic tests (RDTs), and polymerase chain reaction (PCR) [5]. Moreover, microscopy was conducted to detect malaria in asymptomatic pregnant women using the Malaria Rapid Diagnostic (mRDT) method [6]. It takes time to use a microscope, and the availability of parasitologists limits this process [7], The accuracy of diagnosing malaria may be impacted by challenging diagnosis and interpretation as a result of low image quality [8], Technology that can help parasitologists make a diagnosis more quickly and accurately is therefore required [9]. Therefore, equipment that aids in the quicker and more accurate diagnosis of medical professionals or parasitologists is required.

This will facilitate the diagnosis and treatment of malaria patients by parasitologists [10],[11], This study employs Visual Geometry Group (VGG) and deep learning techniques to identify malaria in malaria photos. A variety of deep learning techniques, including CNN, DenseNet, and others, have already identified malaria [12],[13],[14],[15],[16],[17], while prior research employed the fuzzy C-means clustering method, this study applies the thresholding method for segmentation [18], machine learning [19],[20], deep learning [21],[22], fuzzy [23], k-means, channel color space [24],[25], in contrast to other studies that included thresholding, automatically applies the Modified Global

Iranian Journal of Electrical & Electronic Engineering, 2025.
Paper first received 23 Dec 2024 and accepted 22 Feb 2025.
* The author is with the Department of Engineering and Computer Science, Universitas Potensi Utama, Indonesia.
E-mail: edy@potensi-utama.ac.id
** The author is with the Department of Electrical Engineering and Technology, Universiti Malaysia Perlis, Malaysia.
*** The author is with the Department of Medical Microbiology and Parasitology, School of Medical Sciences, Universiti Sains Malaysia, Malaysia.
Corresponding Author: Edy Victor Haryanto S.

Contrast Stretching (MGCS) method to improve image quality [26],[27],[28], contrast stretching [29], HSV [30]. To address these challenges, researchers have explored the use of computer vision and deep learning techniques for automated malaria detection [31]. This research is anticipated to lead to the development of an architectural model that will enhance the precision of diagnosing malaria disease and assist parasitologists in making decisions regarding the treatment and cure of malaria patients. This research aims to create a deep learning model that can accurately detect malaria disease in images, including various conditions and the quality of malaria images.

2 Methodology

Data collecting, picture acquisition, image enhancement, color transformation, segmentation, and classification are some of the stages included in this study. P. falciparum and P. vivax blood smear pictures were obtained from Hospital Universiti Sains Malaysia (HUSM), Department of Medical Microbiology and Parasitology shot at 800 × 600 pixels, and stored in bitmap (*.bmp) format. An OLYMPUS BX41 digital microscope was used to view the blood slides under 100 oil immersion to obtain the thin blood smear pictures in Figure 1. AGCS is used in the picture improvement process to improve contrast, and color transfer to HSV space is the next step. Next, the saturation component is divided using adaptive thresholding, and the Googlenet approach is used for classification.

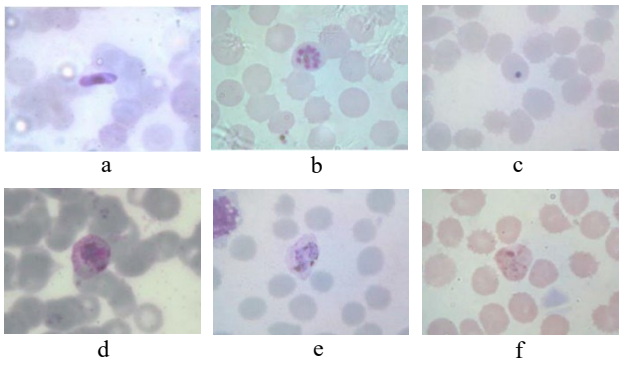

Fig 1. The samples of the captured blood images consisting of (a-c) P.falciparum of thin smear in the gametocyte, schizont, trophozoite; (d-f) P. vivax of thin smear in the gametocyte, schizont, trophozoite.

2.1 Image Enhancement

This study's main innovation is how Adaptive Global Contrast Stretching (AGCS) is used to improve images. In contrast to conventional Global Contrast Stretching (GCS), which involves manually setting the min-max values, AGCS computes these values using the image histogram. To accomplish this automation, the following formulas are used:

Min value computation:

$$minOCR = \min(OCR) - (\max(OCR) - \min(OCR)) \quad (1)$$

Max value computation:

$$maxOCR = \max + (\max(OCR) - \min(OCR)) \quad (2)$$

2.2 Color Transformation

HSV and grayscale color spaces are created from enhanced photos. The new approach is to use the saturation part of HSV, which allows for more accurate segmentation and visualization of malaria parasites than grayscale pictures.

2.3 Image Segmentation

Adaptive thresholding, which is intended to separate the malaria parasites, is the first step in the picture segmentation process.

Where $T_{(x,y)}$ Adaptive threshold value at coordinates (x,y), $\mu_{(x,y)}$, local mean intensity, $\delta_{(x,y)}$ local standard deviation R, dynamic range value (usually 128 for 8-bit pictures), and sensitivity constant k are all included in the thresholding calculation. By adapting dynamically to localized changes in image intensity, this technique improves segmentation accuracy.

2.4 Elimination of Artifacts

Morphological processing and active contour techniques are used to enhance the segmented images. In particular, the 100-iteration Chan-Vese approach is applied. Morphological processes like dilatation and erosion are used

2.5 Segmentation

Only pertinent portions remain when objects with an area smaller than 400 pixels are sorted out. This last stage makes sure that the malaria parasites are accurately and cleanly represented, without any unnecessary noise or artifacts.

2.6 Classification

Currently, the GoogleNet method is being used to build a deep learning model in the form of a new architecture model. This is followed by the training of the deep learning model using collected image data on malaria disease and performance evaluation of the developed model.

3 Result and Discussion

The results of segmentation performance utilizing adaptive thresholding and the elimination of artifacts with morphology and active contour approaches are shown in this section. We applied the adaptive global contrast stretching (AGCS) method for image enhancement.

In the past, global contrast stretching's min-max values had to be manually determined. The bottom 1% and top 1% of all pixel values are specified by the original function in order to determine the boundaries. The precise top and bottom boundaries of the histogram are input into the adjustment function.

Table 1. The Different Between Modified Function and Original

Modified function		Original Function	
Lower limit	Upper limit	Lower limit	Upper limit
0.4863	1.0000	0.6863	0.9725
0.3961	1.0000	0.6157	1.0000
0.5843	1.0000	0.8353	1.0000

A comparison of the original function and the modified function is given in Table 1. In comparison to the higher lower limits of 0.6863, 0.6157, and 0.8353 for the original function, the modified function exhibits a wider enhancement range. This is especially noticeable in the lower limits, which are 0.4863, 0.3961, and 0.5843 for the three cases, respectively. The original function's upper limits are 0.9725, 1.0000, and 1.0000, respectively, whereas the updated function's upper limits are continuously set at 1.0000. This wider range suggests that the altered function is better at highlighting the image's darker areas, which is important for recognizing malaria parasites.

The lowest and maximum values in MGCS are manually set, with 0.1 serving as the minimum and 10 as the maximum. On the other hand, AGCS uses computations based on histogram data to automatically establish these min-max values.

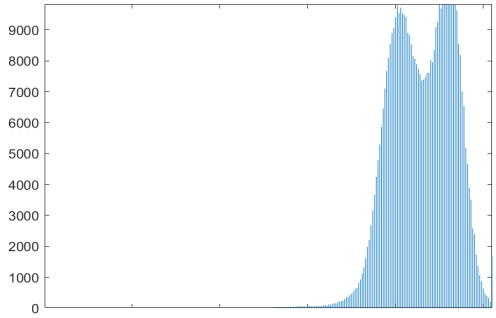

Fig. 2. The example of min - max value on red channel using AGCS

The histogram study into the grayscale picture enhancement utilizing the AGCS method is presented in Figure 2. With intensity levels on the x-axis and their frequency on the y-axis, peaking at about 9000, the histogram shows the distribution of pixel values.

This suggests that there is a notable concentration of higher intensity readings. The Interquartile Range (IQR) is used to generate the automatic min-max values, which are indicated with a minimum value of 0.4863 and a maximum value of 10000. These numbers deviate from the MGCS method's manually determined minmax values, which are fixed at 0.1 and 10, respectively.

Table 2. Value Min Max

	Min	Max
Red Channel	- 0.0275	1.5137
Green Channel	-0.2078	1.6039
Blue Channel	0.1686	1.4157

Table 2 provides valuable insights into the Red, Green, and Blue channel image improvement process using the AGCS approach. The Red channel's maximum value of 1.5137 shows a strong enhancement impact, while the minimum value of -0.0275 indicates a modest adjustment toward negative intensities to boost contrast. With a minimum value of -0.2078 and a high value of 1.6039, the green channel exhibits an even larger adjustment, indicating that it includes crucial information for differentiating features in the photos. The Blue channel shows a significant overall improvement but less adjustment in the lower range of pixel intensities, with a minimum value of 0.1686 and a high value of 1.4157.

Prior to segmentation, the image needs to go through a color alteration following the enhancement method. Grayscale and HSV color channels are the two forms of color transformation that are employed. To get the right input image for the segmentation procedure, this step is essential.

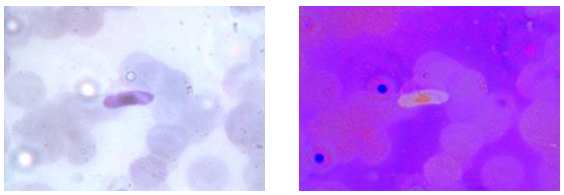

a b

Fig. 3. (a) Malaria image in RGB; (b) malaria image color converted to HSV

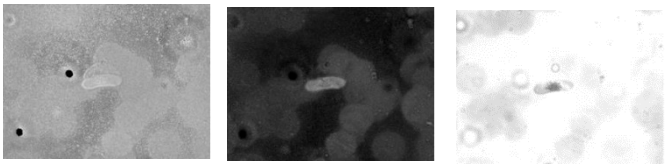

a b c

Fig. 4. (a) color of malaria image in the Hue component; (b) color of malaria image in the Saturation component; and (c) color of malaria image in the value component

In Figure 3, the translation procedure is carried out by transforming the RGB image (Figure 4a) into the HSV color space (Figure 4b). Hue, saturation, and value are the three individual components that make up the HSV

color space, and each one offers a different perspective on the image.

Further exploration of these elements is provided in Figure 4, which shows the malaria image in terms of hue (Figure 4a), saturation (Figure 4b), and value (Figure 4c). The hue component helps distinguish between various elements based on color by highlighting the distinct color kinds that are present, regardless of intensity or saturation. Areas with strong or weak color presence are highlighted by the saturation component, which displays the strength or purity of colors. Last but not least, the value component separates the brightness levels, revealing the distribution of light and changes in intensity throughout the picture.

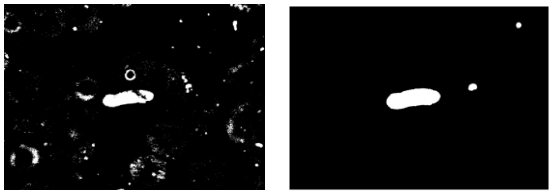

a b

Fig. 5. (a) Result of the segmentation process using adaptive thresholding; (b) Result of artifact elimination through morphological processing

The segmentation procedure used on an input grayscale image is shown in Figure 5. Segmenting the malaria parasites—which show up in the picture as dark areas—is the aim of this procedure. To detect the parasites, the first step in Figure 5(a) is to use adaptive thresholding with a value of 0.5. While the parasites are successfully detected by this method, the final image is heavily noise- and artifact-filled, and the forms of the parasites are not entirely segmented. The following phase entails removing artifacts with morphological processing with a radius of 6 in order to address these difficulties, applying 100 rounds of the Chan-Vese approach

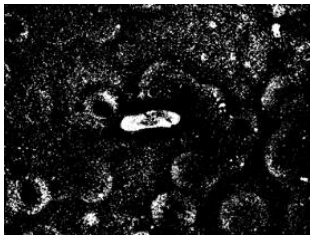

Fig. 6. Result segmentation process with adaptive threshold

The segmentation procedure utilizing the HSV image's saturation component is shown in Figure 6. Segmenting the malaria parasites, which show up in the image as bright areas, is the goal here. To identify the parasites, the first stage entails employing adaptive thresholding with a value of 0.3.

Although the parasites are effectively highlighted by this method, the final image still has a lot of noise and artifacts, and the forms of the parasites are not completely segmented. The next phase entails removing artifacts with morphological processing with a radius of 6 in order to address these difficulties. By reducing noise and artifacts, this procedure enhances segmentation and produces a more accurate depiction of the parasite forms.

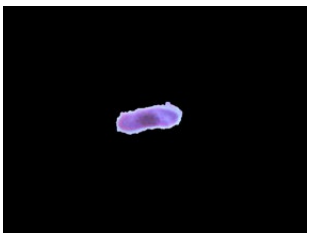

Fig. 7. Result segmentation process final with input saturation component image

After morphological processing to remove artefacts, only important objects are kept. Objects with an area of less than 400 are removed. The result in Figure 8 is a clear image of the malaria parasite with no more artefacts. The final segmentation of Figure 7 uses the input saturation component image to display the shape of the malaria parasite along with the final artefact removal.

The target object's position can be ascertained using the bounds. A grayscale bounding box example. The software was able to identify two target objects in this image. The bounding box for these two target objects has a particular dimension of 224 × 224.

It employed Googlenet deep learning models for the categorization procedure. It utilized 80% of the distribution data for training and 20% for validation.

Table 3. Data for each class HSV training

Class	No. of Data
Artifact	615
PFG	82
PFS	175
PFT	174
PVG	81
PVS	162
PVT	163

Image of the type of malaria used in this study there are two, namely plasmodium falcifarum (PF) and plasmodium vivax (PV), plasmodium falcifarum, there are three stages, namely plasmodium falcifarum gametocyte (PFG), plasmodium falcifarum schizont (PFS) and plasmodium falcifarum thropozoite (PFT) as well as for plasmodium vivax there are three stages namely: plasmodium vivax gametocyte (PVG),

plasmodium vivax schizont (PVS) and plasmodium vivax thropozoite (PVT) as shown in tables 3 and 4.

Table 4. Data for each class HSV validation

Class	No. of Data
Artifact	114
PFG	20
PFS	42
PFT	51
PVG	20
PVS	45
PVT	43

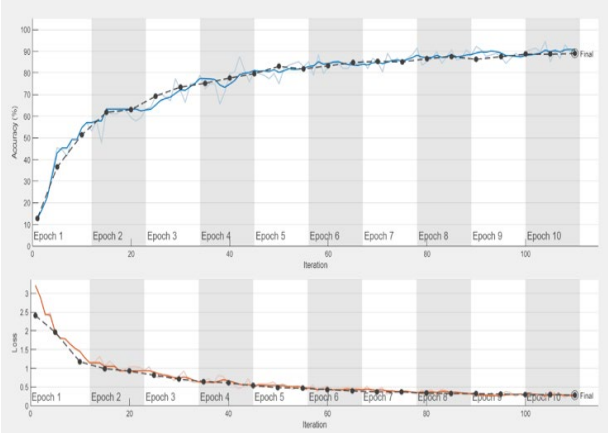

Fig. 8. Result training googlenet process

As seen in Figure 8, the standard deep learning or GoogleNet approach used in this study performs optimally in identifying malaria. The training process using epoch 10 with 100 iterations can produce an accuracy of 88.96% when the validation frequency is used with five iterations. This study uses PC devices with details: Asus motherboard, Intel Core I7-4790 processor, 8 GB RAM, Windows 1.

Table 5. Data for HSV Googlenet Training

Class	Accuracy (%)	Precision	Recall	F1 Score
PFG	99.58	0.93	1.0	0.96
PFS	98.82	0.92	0.99	0.95
PFT	95.71	0.84	0.80	0.82
PVG	99.79	1.0	0.96	0.98
PVS	98.68	0.97	0.91	0.94
PVT	99.31	0.98	0.96	0.97

Table 6. Data for HSV Googlenet Validation

Class	Accuracy (%)	Precision	Recall	F1 Score
PFG	99.1	0.95	0.90	0.92
PFS	96.72	0.84	0.90	0.87
PFT	93.13	0.79	0.75	0.77
PVG	99.4	0.91	1.0	0.95
PVS	97.01	0.93	0.84	0.88
PVT	99.1	0.98	0.95	0.96

Tables 5 and 6 in the training and validation process show that the deep learning method used can work optimally in detecting objects or parasites. The process for detecting or identifying malaria using Googlenet can produce accuracy above 80% using several stages of P. falcifarum and P. vivax.

Table 7. Data for VGG19 Training

Class	Accuracy (%)	Precision	Recall	F1 Score
PFG	99.62	0.96	0.95	0.96
PFS	99.3	0.95	0.98	0.96
PFT	98.22	0.92	0.88	0.90
PVG	99.95	1.0	0.99	0.99
PVS	99.35	0.98	0.95	0.96
PVT	99.68	0.99	0.97	0.98

Table 8. Data for VGG19 Validation

Class	Accuracy (%)	Precision	Recall	F1 Score
PFG	99.34	1.0	0.85	0.92
PFS	99.56	0.98	0.98	0.98
PFT	95.58	0.76	0.86	0.81
PVG	99.56	0.91	1.0	0.95
PVS	99.12	0.94	0.98	0.96
PVT	99.78	1.0	0.98	0.99

Tables 7 and 8 show the results of training and validation using another deep learning method, VGG19. From the tests carried out by the two deep learning methods above the training and validation results, the percentage level of accuracy is not so far from the results, with both being able to detect malaria above 95%.

The analysis of malaria photos is improved by using these several methods, which range from color transformation to adaptive thresholding and morphological processing. Each stage helps to improve particular characteristics and lower noise, which eventually makes it easier to segment and examine malaria parasites in greater detail. In malaria investigations, this methodological approach is crucial for efficient diagnosis and study thus even with artifacts present in the photos utilized for this investigation, the identification procedure can still function effectively.

4 Conclusion

This work shows how to improve blood smear pictures for malaria parasite detection by combining advanced segmentation techniques with Adaptive Global Contrast Stretching (AGCS). The suggested method enables improved visibility and parasite segmentation by transforming the image into HSV color space and concentrating on the saturation component. Adaptive mining is used to produce cleaner, more accurate images by morphological processing, and the Googlenet method

is effective in detecting malaria. This method offers a reliable and scalable solution for malaria detection, which is essential for efficient treatment and lower fatality rates. As such, it solves the shortcomings of previous approaches. The combination of these techniques with automated systems should be investigated in future studies to increase the precision and efficiency of diagnosis.

Conflict of Interest

The authors declare no conflict of interest.

Author Contributions

Edy Victor Haryanto S and **Bob Subhan Riza**: Conceptualization, Methodology & Writing, **Aimi Salihah Abdul Nasir** and **Mohd. Yusoff Mashor**: Analysis, Review Paper & Validation, **Zeehaida Mohamed** : Resource & Data.

Each author has read and agreed to the published version of the manuscript.

Funding

The author would like to acknowledge the support from the International Research Fund Grant Scheme (INTERES) under a grant number of 9008-00039 from the Universiti Malaysia Perlis (UniMAP) and Universitas Potensi Utama.

References

[1] F. Hashmi, S. Aqeel, U. F. Zuberi, and W. Khan, "A systematic review and meta-analysis of inflammatory biomarkers associated with malaria infection and disease severity," *Cytokine*, vol. 169, p. 156305, Sep. 2023, doi: 10.1016/J.CYTO.2023.156305.

[2] A. Requena-Méndez *et al.*, "Malaria parasite prevalence among migrants: a systematic review and meta-analysis," *Clin. Microbiol. Infect.*, vol. 29, no. 12, pp. 1528–1537, Dec. 2023, doi: 10.1016/J.CMI.2023.09.010.

[3] S. H. Khan, N. S. Shah, R. Nuzhat, A. Majid, H. Alquhayz, and A. Khan, "Malaria parasite classification framework using a novel channel squeezed and boosted CNN," *Microscopy*, vol. 71, no. 5, pp. 271–282, 2022, doi: 10.1093/jmicro/dfac027.

[4] V. Reddy, D. J. Weiss, J. Rozier, F. O. ter Kuile, and S. Dellicour, "Global estimates of the number of pregnancies at risk of malaria from 2007 to 2020: a demographic study," *Lancet Glob. Heal.*, vol. 11, no. 1, pp. e40–e47, Jan. 2023, doi: 10.1016/S2214-109X(22)00431-4.

[5] R. Liu *et al.*, "AIDMAN: An AI-based object detection system for malaria diagnosis from smartphone thin-blood-smear images," *Patterns*, vol. 4, no. 9, p. 100806, Sep. 2023, doi: 10.1016/J.PATTER.2023.100806.

[6] G. N. Uyaiabasi *et al.*, "The question of the early diagnosis of asymptomatic and subpatent malaria in pregnancy: Implications for diagnostic tools in a malaria endemic area," *Eur. J. Obstet. Gynecol. Reprod. Biol. X*, vol. 19, no. August, p. 100233, 2023, doi: 10.1016/j.eurox.2023.100233.

[7] S. Saxena, P. Sanyal, M. Bajpai, R. Prakash, and S. Kumar, "Trials and tribulations: Developing an artificial intelligence for screening malaria parasite from peripheral blood smears," *Med. J. Armed Forces India*, Dec. 2023, doi: 10.1016/J.MJAFI.2023.10.007.

[8] S. L. Rei Yan, F. Wakasuqui, and C. Wrenger, "Point-of-care tests for malaria: speeding up the diagnostics at the bedside and challenges in malaria cases detection," *Diagn. Microbiol. Infect. Dis.*, vol. 98, no. 3, p. 115122, Nov. 2020, doi: 10.1016/J.DIAGMICROBIO.2020.115122.

[9] B. E. Fan *et al.*, "From microscope to micropixels: A rapid review of artificial intelligence for the peripheral blood film," *Blood Rev.*, vol. 64, p. 101144, Mar. 2024, doi: 10.1016/J.BLRE.2023.101144.

[10] S. Aqeel, Z. Haider, and W. Khan, "Towards digital diagnosis of malaria: How far have we reached?," *J. Microbiol. Methods*, vol. 204, p. 106630, Jan. 2023, doi: 10.1016/J.MIMET.2022.106630.

[11] G. Akafity, N. Kumi, and J. Ashong, "Diagnosis and management of malaria in the intensive care unit," *J. Intensive Med.*, vol. 4, no. 1, pp. 3–15, Jan. 2024, doi: 10.1016/J.JOINTM.2023.09.002.

[12] M. H. D. Alnussairi and A. A. İbrahim, "Malaria parasite detection using deep learning algorithms based on (CNNs) technique," *Comput. Electr. Eng.*, vol. 103, p. 108316, Oct. 2022, doi: 10.1016/J.COMPELECENG.2022.108316.

[13] D. T. Rademaker *et al.*, "Quantifying the deformability of malaria-infected red blood cells using deep learning trained on synthetic cells," *iScience*, vol. 26, no. 12, p. 108542, Dec. 2023, doi: 10.1016/J.ISCI.2023.108542.

[14] C. Ikerionwu *et al.*, "Application of machine and deep learning algorithms in optical microscopic detection of Plasmodium: A malaria diagnostic tool for the future," *Photodiagnosis Photodyn. Ther.*, vol. 40, p. 103198, Dec. 2022, doi: 10.1016/J.PDPDT.2022.103198.

[15] A. M. Qadri, A. Raza, F. Eid, and L. Abualigah, "A novel transfer learning-based model for diagnosing malaria from parasitized and uninfected red blood cell images," *Decis. Anal. J.*, vol. 9, p. 100352, Dec. 2023, doi: 10.1016/J.DAJOUR.2023.100352.

[16] A. Balaram, M. Silparaj, and R. Gajula, "Detection of malaria parasite in thick blood smears using

deep learning," *Mater. Today Proc.*, vol. 64, pp. 511–516, Jan. 2022, doi: 10.1016/J.MATPR.2022.04.1012.
[17] M. Bhuiyan and M. S. Islam, "A new ensemble learning approach to detect malaria from microscopic red blood cell images," *Sensors Int.*, vol. 4, p. 100209, Jan. 2023, doi: 10.1016/J.SINTL.2022.100209.
[18] J. Somasekar and B. Eswara Reddy, "Segmentation of erythrocytes infected with malaria parasites for the diagnosis using microscopy imaging," *Comput. Electr. Eng.*, vol. 45, pp. 336–351, Jul. 2015, doi: 10.1016/J.COMPELECENG.2015.04.009.
[19] M. Maity, A. Jaiswal, K. Gantait, J. Chatterjee, and A. Mukherjee, "Quantification of malaria parasitaemia using trainable semantic segmentation and capsnet," *Pattern Recognit. Lett.*, vol. 138, pp. 88–94, Oct. 2020, doi: 10.1016/J.PATREC.2020.07.002.
[20] A. de Souza Oliveira, M. Guimarães Fernandes Costa, M. das Graças Vale Barbosa, and C. Ferreira Fernandes Costa Filho, "A new approach for malaria diagnosis in thick blood smear images," *Biomed. Signal Process. Control*, vol. 78, p. 103931, Sep. 2022, doi: 10.1016/J.BSPC.2022.103931.
[21] D. R. Loh, W. X. Yong, J. Yapeter, K. Subburaj, and R. Chandramohanadas, "A deep learning approach to the screening of malaria infection: Automated and rapid cell counting, object detection and instance segmentation using Mask R-CNN," *Comput. Med. Imaging Graph.*, vol. 88, p. 101845, Mar. 2021, doi: 10.1016/J.COMPMEDIMAG.2020.101845.
[22] B. Hemalatha, B. Karthik, C. V. Krishna Reddy, and A. Latha, "Deep learning approach for segmentation and classification of blood cells using enhanced CNN," *Meas. Sensors*, vol. 24, p. 100582, Dec. 2022, doi: 10.1016/J.MEASEN.2022.100582.
[23] S. Chakraborty and K. Mali, "Fuzzy and elitist cuckoo search based microscopic image segmentation approach," *Appl. Soft Comput.*, vol. 130, p. 109671, Nov. 2022, doi: 10.1016/J.ASOC.2022.109671.
[24] S. Edy Victor Haryanto, M. Y. Mashor, A. S. A. Nasir, and Z. Mohamed, "Identification of Giemsa Staind of Malaria Using K-Means Clustering Segmentation Technique," in *2018 6th International Conference on Cyber and IT Service Management, CITSM 2018*, 2019. doi: 10.1109/CITSM.2018.8674254.
[25] S. E. V. Haryanto, M. Y. Mashor, A. S. A. Nasir, and H. Jaafar, "A fast and accurate detection of Schizont plasmodium falciparum using channel color space segmentation method," in *2017 5th International Conference on Cyber and IT Service Management, CITSM 2017*, Institute of Electrical and Electronics Engineers Inc., Oct. 2017. doi: 10.1109/CITSM.2017.8089290.
[26] S. Dash *et al.*, "Guidance Image-Based Enhanced Matched Filter with Modified Thresholding for Blood Vessel Extraction," *Symmetry (Basel).*, vol. 14, no. 2, pp. 1–19, 2022, doi: 10.3390/sym14020194.
[27] T. A. Aris, A. S. A. Nasir, W. A. Mustafa, M. Y. Mashor, E. V. Haryanto, and Z. Mohamed, "Robust Image Processing Framework for Intelligent Multi-Stage Malaria Parasite Recognition of Thick and Thin Smear Images," *Diagnostics 2023, Vol. 13, Page 511*, vol. 13, no. 3, p. 511, Jan. 2023, doi: 10.3390/DIAGNOSTICS13030511.
[28] H. A. Nugroho and R. Nurfauzi, "A combination of optimized threshold and deep learning-based approach to improve malaria detection and segmentation on PlasmoID dataset," *FACETS*, vol. 8, no. 1, pp. 1–12, Aug. 2023, doi: 10.1139/FACETS-2022-0206.
[29] R. Rosnelly, B. S. Riza, L. Wahyuni, S. Suparni, A. Prasetio, and R. Rahim, "Improvement of Hybrid Image Enhancement for Detection and Classification of Malaria Disease Types and Stages with Artificial Intelligence," *TEM J.*, vol. 11, no. 2, pp. 535–542, 2022, doi: 10.18421/TEM112-06.
[30] W. M. Fong Amaris, C. Martinez, L. J. Cortés-Cortés, and D. R. Suárez, "Image features for quality analysis of thick blood smears employed in malaria diagnosis," *Malar. J.*, vol. 21, no. 1, pp. 1–12, 2022, doi: 10.1186/s12936-022-04064-2.
[31] Q. A. Arshad *et al.*, "A dataset and benchmark for malaria life-cycle classification in thin blood smear images," *Neural Comput. Appl.*, vol. 34, no. 6, pp. 4473–4485, 2022, doi: 10.1007/s00521-021-06602-6.

Biographies

Edy Victor Haryanto S is with the Department of Informatics, Faculty of Engineering and Computer Science, Universitas Potensi Utama, Medan, Indonesia. He has about 8 years of experience in teaching and research. He has several publications in international journals. His areas of interest are Digital Image Processing and Artificial Intelligence.

Dr. Aimi Salihah Abdul Nasir received her B.Eng (Hons) degree in Mechatronic Engineering from Universiti Malaysia Perlis (UniMAP) in 2009. In 2015, she obtained her Ph.D. in Biomedical Electronic Engineering from the same university, specialized in medical image processing with a focus on clustering analysis. Her research interests include image processing, artificial intelligence, and deep learning.

Prof. Dr. Mohd Yusoff Mashor obtained his Bachelor of Engineering in Control and Computer Engineering from University of Westminster, London in 1990. Under Universiti Sains Malaysia (USM) RLKA scheme, he pursued his M.Sc in Control Engineering and Information Technology at University of Sheffield in 1991. In 1995, he obtained his PhD specialized in neural network from the same university. He started his service in USM in the School of Electrical and Electronic Engineering in December 1995. He is currently the Dean of Postgraduate Studies, Universiti Malaysia Perlis. Since his PhD time, he is actively involved in research. Over the years, he has developed his expertise in neural network, system identification, fuzzy logic, control system, intelligent forecasting/prediction, image processing and medical diagnostic systems. He has authored and co-authored for more than 100 research publications in the form of book chapters, refereed journals and conferences at the international and national levels.

Dr. Bob Subhan Riza, ST, M.Kom was born in Medan, North Sumatra on August 5, 1970. As for my Educational History, - D3 at USU Medan Polytechnic graduated in 1993 - S1 at the University of N orth Sumatra, Medan graduated in 2000 - S2 at Putera Indonesia University YPTK Padang graduated in 2014. S3 Information Technology at Putera Indonesia University YPTK Padang graduated in 2023. Currently I am serving as a Permanent Lecturer at Universitas Potensi Utama. My research study in the field of Image Processing.

Prof. Dr. Zeehaida Mohamed, MD (UKM), Master of Pathology (Medical Microbiology) (USM), is a dedicated Clinical Microbiologist at Hospital Universiti Sains Malaysia. With a strong background in medical microbiology, she has a profound interest in research focusing on microbiology and medical parasitology. Her work contributes to advancing diagnostic and clinical practices, particularly in infectious diseases, with a commitment to improving patient outcomes through innovative research and laboratory expertise.